Environ. Sci. Technol. **2004**, *38,* 2175−2181

Tracing Atmospheric Nitrate Deposition in a Complex Semiarid Ecosystem Using $\Delta^{17}O$

GREG MICHALSKI,*,† THOMAS MEIXNER,‡ MARK FENN,§ LARRY HERNANDEZ,† ABBY SIRULNIK,‡ EDITH ALLEN,‡ AND MARK THIEMENS†

University of California, San Diego, La Jolla, California 92095-0356, University of California, Riverside, Riverside, California 92521, PSW Research Station, USDA Forest Service, Riverside, California 92507

The isotopic composition of nitrate collected from aerosols, fog, and precipitation was measured and found to have a large ^{17}O anomaly with $\Delta^{17}O$ values ranging from 20‰ to 30‰ ($\Delta^{17}O = \delta^{17}O - 0.52(\delta^{18}O)$). This ^{17}O anomaly was used to trace atmospheric deposition of nitrate to a semiarid ecosystem in southern California. We demonstrate that the $\Delta^{17}O$ signal is a conserved tracer of atmospheric nitrate deposition and is a more robust indicator of N deposition relative to standard $\delta^{18}O$ techniques. The data indicate that a substantial portion of nitrate found in the local soil, stream, and groundwater is of atmospheric origin and does not undergo biologic processing before being exported from the system.

Introduction

The global nitrogen cycle has been altered by human activities such that human N_2 fixation annually more than doubles natural fixation, and this N flux is expected to again double by 2030 (*1*−*3*). The negative impacts of excess N input include shifts in biodiversity (*4*), soil acidification and forest decline (*5*), eutrophication of coastal waters and estuaries (*6*), and degradation of groundwater and surface water (*7, 8*). Nitrogen originating from combustion of fossil fuel has the unique potential to impact ecosystems far from their source including pristine wilderness preserves (*5*). The direct contribution of atmospheric N to N export is difficult to ascertain, but is estimated to vary from 10% to 50% (*6*). Transport of atmospheric fixed N pollutants across local, regional, and national boarders also raises questions on how emission reduction strategies should be implemented by local authorities.

Nitrate is a unique form of fixed N because of its high solubility, which allows it to be leached and exported out of ecosystems. This export often leads to accumulation of NO_3^- in groundwater, and EPA regulations dictate that potable water NO_3^- concentrations must not exceed 10 ppm. Atmospheric NO_3^- ($NO_3^-{}_{atm}$) is a mixture of gas-phase nitric acid, produced by the oxidation of NO_x, and NO_3^- salts formed by heterogeneous reactions involving NO_y on aerosol surfaces (*9*). The main removal mechanism of $NO_3^-{}_{atm}$ is through dry and wet deposition, and it can be a substantial source of new N, but its utilization by biota depends largely on the N retention dynamics of the system in question. Researchers have recently applied $\delta^{18}O$ and $\delta^{15}N$ methods (*10*) to determine the fate and transport of $NO_3^-{}_{atm}$ to ecosystems, but there are significant limitations to the effectiveness of this methodology. Because of the wide range of observed $\delta^{18}O$ and $\delta^{15}N$ values for the two main sources of NO_3^-, microbial nitrification of organic matter and $NO_3^-{}_{atm}$, it is difficult to detect and quantify $NO_3^-{}_{atm}$ deposition in natural systems using isotopic mass balance (*11*−*13*). In addition, kinetic and equilibrium isotopic fractionation processes, such as denitrification and abiotic reductions, can alter NO_3^- $\delta^{18}O$ and $\delta^{15}N$ values, complicating their interpretation beyond the simple isotope mass balance approach (*11*).

Recent observations have shown that $NO_3^-{}_{atm}$ is anomalously enriched in ^{17}O (*13*). Such enrichments are generally quantified by $\Delta^{17}O$ notation, $\Delta^{17}O = \delta^{17}O - 0.52(\delta^{18}O)$, where $\delta = (R_{sample}/R_{standard} - 1) \times 1000$ and R is the $^{17}O/^{16}O$ or $^{18}O/^{16}O$ ratio of the sample and the standard. The origin and seasonal variation in the observed $\Delta^{17}O$ of $NO_3^-{}_{atm}$ is attributed to oxygen atom transfers from ozone (where the $\Delta^{17}O$ is well characterized (*14, 15*)) to oxides of nitrogen during the conversion of NO_x to $NO_3^-{}_{atm}$ (*13*). Because the production of nonzero $\Delta^{17}O$ values is strictly a photochemical effect, NO_3^- produced in soils by nitrification has $\Delta^{17}O = 0$. Furthermore, postdepositional isotopic fractionations such as denitrification will obey the well-established mass-dependent fractionation law $\delta^{17}O = 0.52(\delta^{18}O)$ (*16*), leaving the $\Delta^{17}O$ unaltered. Therefore, $\Delta^{17}O$ can be used as a conserved tracer of $NO_3^-{}_{atm}$ deposition. Hydrologists, ecologists, and soil scientists can use such a tracer to better understand the fate of atmospheric deposition.

Here we demonstrate the effectiveness of using $\Delta^{17}O$ for detecting and quantifying the proportion of $NO_3^-{}_{atm}$ found in NO_3^- that was collected from streams and soils along a pollution gradient in southern California. Additionally we use these results to gain insight into the processes controlling the fate and transport of nitrogen in the soil and catchment environments.

Experimental Section

Site Description. We sampled nitrate in streams, soils, zero-tension soil lysimeters, and atmospheric pollutants along two air pollution gradients in southern California (Figure 1). Each receives at least 35−45 kg of N ha^{-1} yr^{-1} on the northwest end nearest Los Angeles and roughly 5 kg of N ha^{-1} yr^{-1} at the southeast terminus furthest from the city (*17*−*19*). This nitrogen deposition has been implicated in the recent decline of the coastal sage scrub ecosystems of southern California (*20, 21*) and is linked to elevated NO_3^- concentrations in local streams (*22, 23*).

Streamwater, fog, and wet deposition samples were collected from the San Dimas Experimental Forest, a low-elevation high-pollution chaparral site in the San Gabriel Mountains northeast of Los Angeles. Streamwater samples were also collected in the Devil Canyon watershed (high N deposition site), also predominantly chaparral vegetation, located on the western edge of the San Bernardino Mountains (Figure 1). Camp Paivika is a high-pollution mixed-conifer site located at the crest of Devil Canyon. At Camp Paivika nitrate samples were obtained from soil, soil lysimeters, fog, and wet deposition.

Study sites with relatively low or moderate levels of N deposition included Camp Osceola and Barton Flats located near the eastern end of the mixed-conifer zone in the San Bernardino Mountains, where N deposition is 5−7 times

* Corresponding author phone: (858) 534-6053; fax: (858) 534-7042; e-mail: gmichalski@ucsd.edu.
† University of California, San Diego.
‡ University of California, Riverside.
§ USDA Forest Service.

10.1021/es034980+ CCC: $27.50
Published on Web 03/03/2004

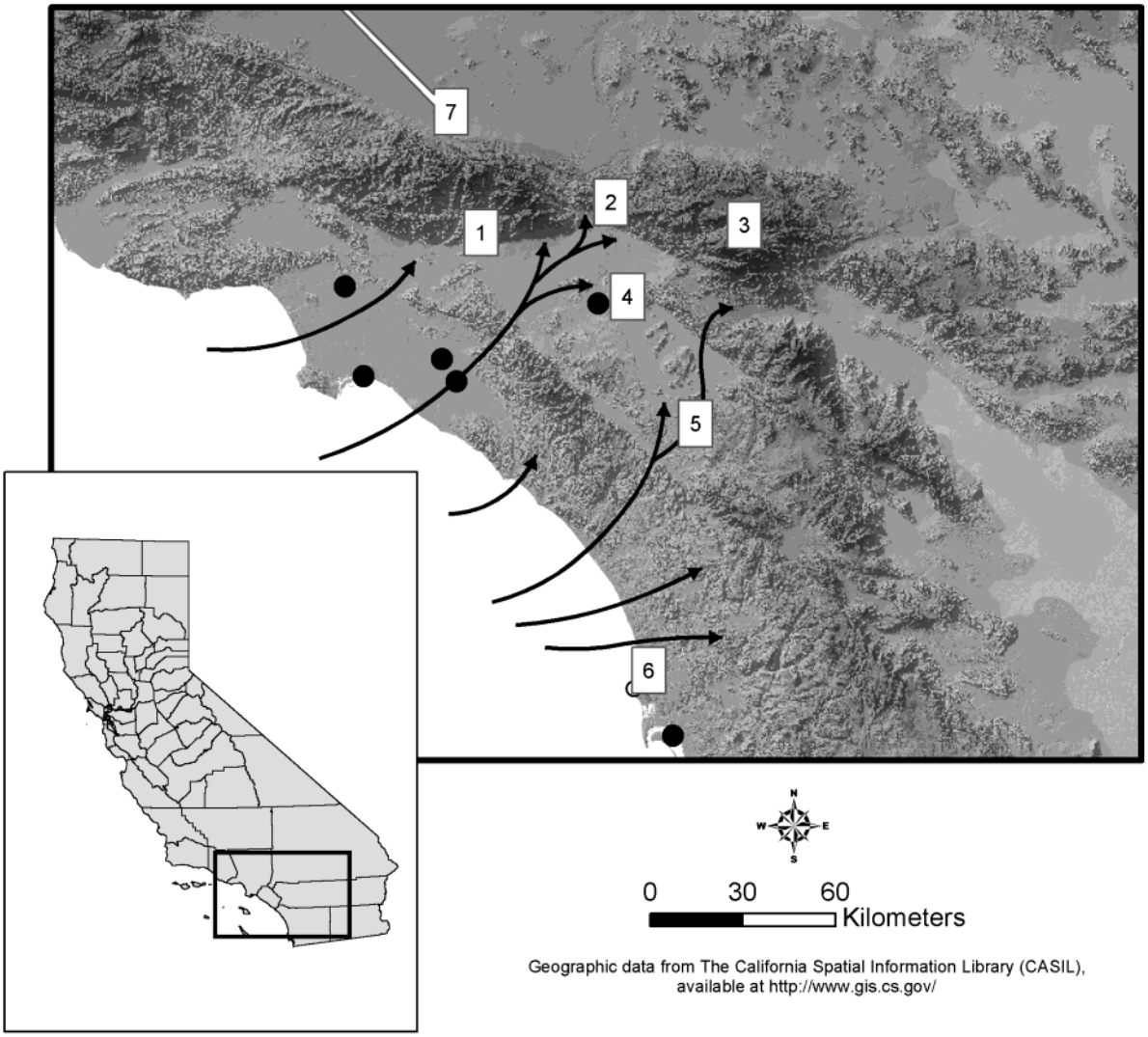

FIGURE 1. The mountain gradient (proceeding from 1 to 3) begins 30 km northeast of Los Angeles in the San Gabriel Mountains (1), which contains the Camp Paivika/Devil Canyon watershed (2) and reaches to the eastern end of the San Gorgonio wilderness (3) in the San Bernardino Mountains, 130 km east of Los Angeles. Both of these sites are dominated by mixed-conifer forest at high elevations and change to chaparral vegetation at lower elevations. The valley gradient (from 1 to 5), predominantly coastal sage scrub habitat, begins in Riverside, CA (4), and ends near Lake Skinner (5) (100 km). La Jolla (6) is approximately 140 km southwest and Bakersfield (7) 160 km northwest of the gradients. Atmospheric samples were collected at these last two sites in addition to the Riverside, CA, location.

lower than at Camp Paivika. Both soil and fog samples at these two sites were obtained for nitrate analysis. Streamwater samples were also collected from creeks at the southern edge of the San Gorgonio Wilderness (moderate N deposition) (Figure 1). Two additional field sites were located in the coastal sage scrub ecotone of southern California. One is situated on the campus of the University of California, Riverside (UCR), and the other is located at the Lake Skinner conservation reserve. The UCR site is subject to high rates of deposition, and the Lake Skinner site is a lower deposition site. At both sites, only soils were sampled, as streamflow is rare and was not observed during the study period.

NO_3^- Collection and Analysis. Each sample ultimately ends up as a dilute aqueous solution of soluble anions (Cl^-, NO_3^-, and SO_4^{-2}) and dissolved organic material. The organics are removed and the anions concentrated on 5 mL anion resin columns (Bio-Rad AG1-X8 200−400 mesh) as described by Silva et al. (2000). After loading, all resin columns were kept at 5 °C prior to isotopic analysis. The $NO_{3\,atm}^-$ samples were collected as precipitation, fog, and aerosols. The precipitation collections utilized Aerochem wet/dry bucket samplers following guidelines detailed by the National Atmospheric Deposition Program (NADP). Fogwater was collected by actively pulling the fog through a bank of Teflon collector strings that funnel the droplets into precleaned Nalgene bottles (*24*). Aerosol NO_3^- was collected for 3 days on precleaned glass fiber filters using a high-volume aerosol sampler (flow rate 1200 L min^{-1}) equipped with a four-stage, size-segregating impactor. Aerosol samples were collected in La Jolla, CA, a coastal urban site, Riverside, CA, an inland urban center near UCR, and Bakersfield, CA, a suburban farming community in the California central valley (Figure 1). The aerosol samples are considered a mixture of aerosol $NO_{3\,atm}^-$ and gaseous HNO_3 because HNO_3 is known to react with material on the filter surface to form nitrate salts (*25*). The soluble salts were extracted by repeatedly sonicating the filters in 50 mL of Millipore water.

Streamwater samples were collected in the field in clean, triply rinsed Nalgene sample bottles. Water samples were filtered (0.45 μm pore size) within 2 days following field collection. Soils were sampled at several depth intervals down to 30 cm below the surface, including the litter layer of the soil profile. Soil samples were stored frozen prior to extraction. Soluble ions were extracted from the soils by mixing them in a 1:10 ratio with Millipore water and shaken for 2 h. The soil extracts were then centrifuged, filtered through a 0.45

TABLE 1. Selected Stream, Soil, and Lysimeter NO_3^- Isotopic and Concentration Data[a]

sampling location/type	date	$[NO_3^-]$ (μmol of N/L)	$\delta^{18}O$	$\delta^{17}O$	$\Delta^{17}O$	% $NO_3^-{}_{atm}$ $\Delta^{17}O$	% $NO_3^-{}_{atm}$ $\delta^{18}O$
stream base flow							
San Gorgonio	2/7/01		23.3	12.8	0.7	3.1	29.8
San Dimas	2/25/01		16.8	10.5	1.7	7.2	18.7
Devil Canyon 2	2/7/01	69	13.4	8.8	1.8	7.7	12.7
Devil Canyon 5	3/13/01	240	32.6	18.8	1.8	7.6	45.9
storm flow							
San Gorgonio 1	7/5/01		9.3	9.9	5.1	21.1	5.7
San Gorgonio 3	3/18/02		11.4	10.7	4.7	19.7	9.3
Devil Canyon 7	11/13/01	206	29.6	23.9	8.5	35.2	40.7
Devil Canyon 2	11/13/01	250	20.7	19.1	8.4	34.8	25.4
Devil Canyon 7	3/17/02	100	30.4	24.7	8.9	37.2	42.1
Devil Canyon 2	3/17/02	80	34.0	27.5	9.8	40.7	48.3
zero tension soil lysimeter							
Camp Pavika lysimeter 6B	5/2/01	522	−24.8	-8.9	4.0	16.5	0.0
Camp Pavika lysimeter 6C	5/2/01	370	22.4	15.4	3.8	15.7	28.2

sampling location/type	date	$[NO_3^-]$ (μmol of N/g of soil)	$\delta^{18}O$	$\delta^{17}O$	$\Delta^{17}O$	% $NO_3^-{}_{atm}$ $\Delta^{17}O$	% $NO_3^-{}_{atm}$ $\delta^{18}O$
soil extracts							
Camp Paivika surface litter	10/25/01	110	58.5	49.3	18.9	78.9	90.5
Camp Paivika 0−2 cm	10/25/01	47	21.5	13.7	2.5	10.5	26.7
Camp Paivika 2−10 cm	10/25/01	69	20.6	13.4	2.7	11.4	25.1
Camp Paivika 20−30 cm	10/25/01	52	15.7	10.8	2.6	11.0	16.7
Lake Skinner 0−2 cm	3/18/02	19	7.4	4.3	0.5	1.9	2.4
Lake Skinner 2−10 cm	3/18/02	24	4.0	3.7	1.6	6.7	0.0
Lake Skinner 20−30 cm	5/8/02	16	6.3	4.2	0.9	3.8	0.5
CAO tree 1 2−10 cm	5/8/02	7.35	18.4	10.1	0.5	2.1	21.4
CAO tree 5 20−30 cm	5/8/02	7.3	13.9	8.2	1.0	4.0	13.7

[a] Percentage of $NO_3^-{}_{atm}$ estimates are determined using $\delta^{18}O$ = 70‰ and $\Delta^{17}O$ = 25‰ as average $NO_3^-{}_{atm}$ values.

μm filter, and stored in the dark at 4 °C until ready for concentration onto anion resin columns.

The anions were eluted from the column, and the NO_3^- was purified and converted to $AgNO_3$ as described by Silva et al. For samples with high loads of dissolved organics carbon (DOC), the eluent was further purified by SPE using C-18 resin and by anion separation using a high-capacity ion chromatograph (*26*). The $AgNO_3$ was freeze-dried directly in silver capsules, converted to O_2, and analyzed for $\delta^{17}O$ and $\delta^{18}O$ using a duel-inlet Finnigan-Mat isotope ratio mass spectrometer (*26*). All oxygen isotopic data presented are measured with respect to SMOW and have accuracy and precision of ±1.5‰ for $\delta^{18}O$ and ±0.2‰ for $\Delta^{17}O$ (*26*).

Results and Discussion

Oxygen Isotopic Composition of Atmospheric Nitrate. The oxygen isotopic compositions of the $NO_3^-{}_{atm}$ samples are plotted in an oxygen three-isotope space, and shows the large ^{17}O isotope enrichments relative to the terrestrial isotopic mass fractionation line (Figure 2). The average $NO_3^-{}_{atm}$ $\Delta^{17}O$ value is 26‰ with a spread of ±3‰ and is in the same range as previously reported $NO_3^-{}_{atm}$ $\Delta^{17}O$ values. We have also included, in Figure 2, the $NO_3^-{}_{atm}$ $\Delta^{17}O$ results from our previous study (La Jolla) (*13*) to give a clear representation of the range of $\Delta^{17}O$ values observed. In that study the $\Delta^{17}O$ values for $NO_3^-{}_{atm}$ were modeled by tracing NO_x oxidation pathways that shifted depending on the season and oxidant species. Those results showed that the $NO_3^-{}_{atm}$ formed during the winter months had consistently higher $\Delta^{17}O$ values than $NO_3^-{}_{atm}$ produced in the spring or summer. The precipitation and aerosol samples from Riverside and Bakersfield were predominately collected during the winter when the $\Delta^{17}O$ values in $NO_3^-{}_{atm}$ are highest. This bias of predominately winter sampling in this study only overestimates the average $NO_3^-{}_{atm}$ $\Delta^{17}O$ by about 1‰, and we have taken the annual average $NO_3^-{}_{atm}$ $\Delta^{17}O$ as ~25‰.

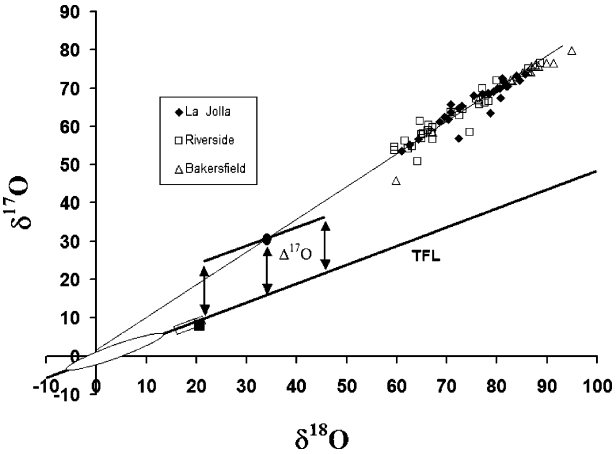

FIGURE 2. Oxygen three isotope plot of $NO_3^-{}_{atm}$ from the Riverside Air Basin (□), La Jolla, CA (◆), and Bakersfield, CA (△), showing an average $\Delta^{17}O$ of 25 ± 4 ‰ and a high correlation between $\delta^{17}O$ and $\delta^{18}O$. The solid bold line is the terrestrial fractionation line (TFL) that describes most nonphotochemical isotopic compositions ($\delta^{17}O = 0.52(\delta^{18}O)$) including NO_3^- from nitrification (white oval), fertilizer NO_3^- (open rectangle), and air O_2 (solid square). Mixing between $NO_3^-{}_{atm}$ and NO_3^- from nitrification or fertilizer decreases the $\Delta^{17}O$ proportionally to the respective source strengths (solid circle). Once mixed, any subsequent kinetic or equilibrium isotopic fractionations (denitrification/reduction) follow $\delta^{17}O = 0.52(\delta^{18}O)$, i.e., parallel to the terrestrial fractionation line, leaving the $\Delta^{17}O$ unaltered (arrows). Our overall $NO_3^-{}_{atm}$ $\delta^{18}O$ values are larger (60−95‰) than those of other studies (40−75‰) but with similar spreads (35‰) and are likely due to recent evidence showing offline NO_3^- $\delta^{18}O$ experimental methods suffer from scaling factors for samples that differ significantly from $\delta^{18}O$ near 23‰ (*30*).

The $NO_3^-{}_{atm}$ $\delta^{18}O$ values are also highly enriched and are in reasonable agreement with $\delta^{18}O$ values reported for nitrate

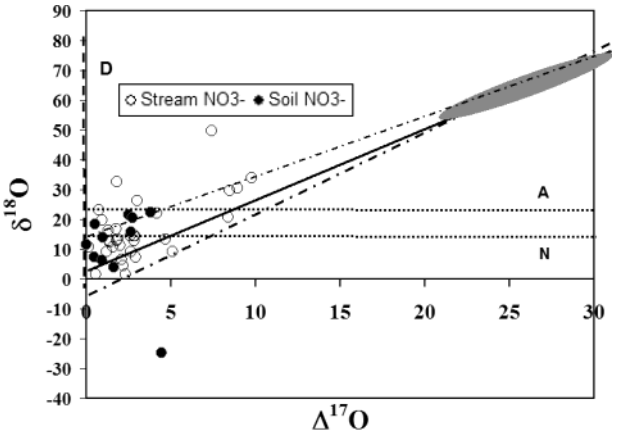

FIGURE 3. NO_3^- from stream (○) and soil (●) samples and $\delta^{18}O$ and mass balance mixing lines between $NO_3^-{}_{atm}$ (solid oval) and nitrification NO_3^-. Nitrification utilizes O atoms from atmospheric O_2 ($\delta^{18}O = 23.5‰$, $\Delta^{17}O = -0.15‰$) and soil water in a 1:2 ratio (*21*). Precipitation (H_2O) for this study had $\delta^{18}O = -8 \pm 0.3‰$ and $\Delta^{17}O = 0$, which would result in a nitrification $\delta^{18}O \approx +3‰$ and $\Delta^{17}O \approx -0.1‰$ (*y*-axis terminus of the solid line), assuming no isotopic fractionation occurs when O_2 diffuses into the soil. Other studies indicate the O_2/H_2O ratio shifts with changing conditions and can produce NO_3^- with $\delta^{18}O$ values ranging from −5‰ to +15‰ (*y*-axis terminus of the dotted−dashed lines) (*21*, *24*). $NO_3^-{}_{atm}$ detection limits using $\delta^{18}O$ are shown as horizontal dotted lines for natural systems (N) where nitrification and $NO_3^-{}_{atm}$ are the only NO_3^- sources and for agricultural regions (A) where fertilizer NO_3^- ($\delta^{18}O \approx 18-23‰$, $\Delta^{17}O \approx -0.2$) is an additional source. Points above these lines are considered to have detectable $NO_3^-{}_{atm}$. The detection limit using $\Delta^{17}O$ (vertical dashed line, D) is based on our analytical precision/accuracy of 0.2‰, with points to the right of the line being samples with detectable $NO_3^-{}_{atm}$.

in wet deposition (*10*, *11*, *27*). Since the $\Delta^{17}O$ enrichments in $NO_3^-{}_{atm}$ are the result of NO_x oxidation by ozone (*13*, *28*), which is equally enriched in both ^{17}O and ^{18}O (*29*), during its conversion to HNO_3, it is not surprising to find the $\delta^{18}O$ values following trends similar to those of the $\Delta^{17}O$ values. The higher variability observed in $NO_3^-{}_{atm}$ $\delta^{18}O$ values is likely the result of fluctuations in the $\delta^{18}O$ tropospheric water vapor, which is incorporated into $NO_3^-{}_{atm}$ during heterogeneous hydrolysis and the $NO_2 + OH \rightarrow HNO_3$ reaction (*13*). Kinetic isotope effects for the numerous reactions involved in the NO_x cycle may also be playing a role in the $\delta^{18}O$ variability. It is unlikely the fluctuating $\delta^{18}O$ values are the signature of multiple NO_x sources as previously suggested (*11*), since industry and emission do not radically vary with season in the Los Angles basin. Rather, the $\delta^{18}O$ variations are also the result of shifts in oxidation chemistry (the increased importance of N_2O_5 hydrolysis) that vary with sunlight, temperature, and oxidant levels (*13*).

Oxygen Isotopic Composition of Stream and Soil NO_3^-. All soil and aquatic NO_3^- samples in this study had positive $\Delta^{17}O$ values (Table 1, Figure 3), unambiguously showing that every sample of soil and water has some degree of $NO_3^-{}_{atm}$ input. This result is in stark contrast to detecting $NO_3^-{}_{atm}$ deposition using the $\delta^{18}O$ methodology, which would indicate only 15−30% of the samples had detectable $NO_3^-{}_{atm}$ (Figure 3). The correlation between $\Delta^{17}O$ and $\delta^{18}O$ values observed in the atmospheric samples (Figure 2) is absent in the terrestrial samples (Figure 3), showing that while $\Delta^{17}O$ scales with the degree of $NO_3^-{}_{atm}$ deposition, some unknown processes are affecting the $\delta^{18}O$ values. The divergence may be due to variability of microbial NO_3^- $\delta^{18}O$ values that can range from −5 to +15‰ depending on isotopic composition of the pore water and O_2, soil characteristics, pH, N speciation, and bacterial species (*12*). These factors require that the microbial $\delta^{18}O$ end member be determined by in situ experiments at each individual site. The $\Delta^{17}O$ is zero for all microbial nitrification because the oxygen reservoirs utilized in nitrification are water and atmospheric O_2, which both have measured $\Delta^{17}O$ of ~0, and the nitrification process itself is a mass-dependent process. Therefore, no knowledge of the soil conditions or the isotopic composition of the pore water or pore O_2, both of which have variable $\delta^{18}O/\delta^{17}O$ values, need be known to apply $\Delta^{17}O$ for estimating $NO_3^-{}_{atm}$ deposition.

$\delta^{18}O$ alterations may also result from known mass-dependent isotopic fractionations such as denitrification (*11*) or the effect of unmeasured processes, such as soil uptake, plant utilization, abiotic reductions, and ionic transport. For example, isotopic discrimination during leaching has been suggested as one of the causes in the observed $\delta^{15}N$ enrichments with depth in soil NO_3^- profiles. Similar increases in the $\delta^{18}O$ values of leached NO_3^- would be expected (they have yet to be determined) in roughly a 2:1 fashion relative to $\delta^{15}N$ values, in a manner similar to the 2:1 $\delta^{18}O$:$\delta^{15}N$ enrichments observed in denitrifying conditions (*11*). Although such processes will also alter the $\delta^{17}O$ (in conjunction with $\delta^{18}O$), they do so in a mass-dependent manner, which on a three-isotope plot generates an array of slope 0.52 parallel to, but offset from, the terrestrial mass fractionation line and leaves the $\Delta^{17}O$ unchanged (see Figure 2). This emphasizes that although the $\Delta^{17}O$ calculations are made relative to $\delta^{18}O$ values, they are independent of the absolute $\delta^{18}O$ value. For example, the NO_3^- found the Devil Canyon streams during base flow have $\delta^{18}O$ values that differ by 20‰ but have identical $\Delta^{17}O$ values (Table 1).

The variability in the isotopic composition of the biologic end member and fractionation dynamics have been previously cited as the limiting factors in the quantifying $NO_3^-{}_{atm}$ deposition budgets using $\delta^{18}O$ (*12*). The consequence of these fractionating processes for quantifying $NO_3^-{}_{atm}$ loads can be seen in a comparison of $\delta^{18}O$ and $\Delta^{17}O$ mass balance approaches (Figure 4). Both overestimations and underestimations of $NO_3^-{}_{atm}$ are prevalent in the $\delta^{18}O$ data, calling into question recent studies that indicate $NO_3^-{}_{atm}$ is not relevant even in watersheds with high N deposition (*31*). These percentage estimates of $NO_3^-{}_{atm}$ are relative to the terrestrial NO_3^- sources, and local $\Delta^{17}O$ fluctuations (within each site) are more likely due to the varying local importance of nitrification rather than deposition differences. Nitrification includes both nitrification of mineralized plant N and the nitrification of NH_4^+ that is derived from atmospheric deposition, and it is not possible to distinguish between the two N sources using current isotopic methods. The study areas presented here have NH_4^+ deposition of roughly equal importance relative to NO_3^- deposition (*32*, *33*) so that any N deposition estimates based on $NO_3^-{}_{atm}$ ($\Delta^{17}O$) are at least a factor of 2 too low. In addition, because the nitrification of atmospheric NH_4^+ will have a $\Delta^{17}O = 0$, our N deposition estimates based on $\Delta^{17}O$ calculations may be further diluted, so caution must be used when total N is extrapolated from $NO_3^-{}_{atm}$.

The advantages of the $\Delta^{17}O$ methodology for identifying the fraction of $NO_3^-{}_{atm}$ present are shown by looking at the results from the soil and stream transect sites. At sites closest to Los Angeles, nitrate extracted from surface litter is almost exclusively $NO_3^-{}_{atm}$, with the underlying soil containing up to 17% $NO_3^-{}_{atm}$ and significant amounts of $NO_3^-{}_{atm}$ detectable throughout the soil profile and in soil lysimeter extracts (Table 1). Soils from the less polluted sites generally contained less than half the amount of $NO_3^-{}_{atm}$ relative to the polluted sites even though the deposition rate is a factor of 5 smaller at this locale, which suggests that nitrification rates are more dominant in this region. The preservation of the soil nitrate $\Delta^{17}O$ signal indicates that $NO_3^-{}_{atm}$ in soils did not undergo complete biological processing prior to being leached from

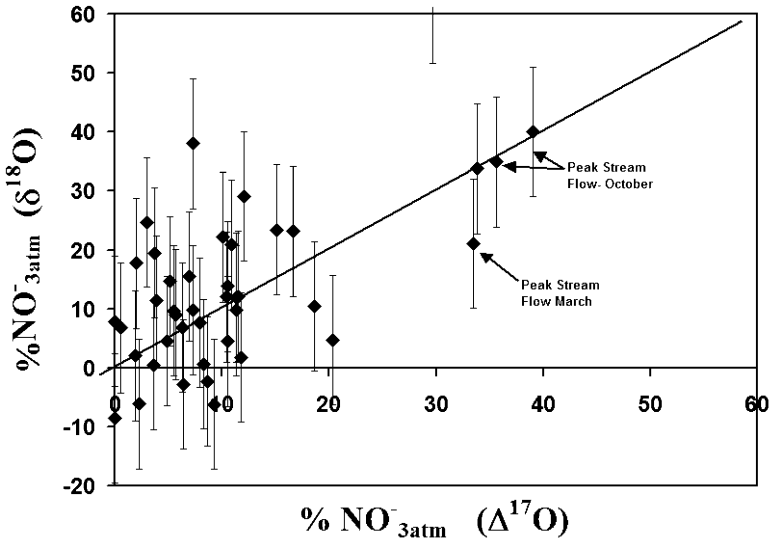

FIGURE 4. Mass balance estimates of the percentage of $NO_3^-{}_{atm}$ in terrestrial NO_3^- samples using an average $NO_3^-{}_{atm}$ $\delta^{18}O = 70‰$ and $\Delta^{17}O = 25‰$ and a nitrification NO_3^- $\delta^{18}O$ of 3‰, $\Delta^{17}O = -0.1$. The solid line is a 1:1 correlation slope if the $\delta^{18}O$ method and the $\Delta^{17}O$ method gave the same percentage of $NO_3^-{}_{atm}$. Error bars represent uncertainties using solely the $\delta^{18}O$ values due to the range of possible nitrification $\delta^{18}O$ values from −5‰ to +15‰. Zero or negative percent would be interpreted as having no $NO_3^-{}_{atm}$. Peak streamflow during the October storm results in good agreement between $\delta^{18}O$ and $\Delta^{17}O$ methods. No correlation exists in later storms (March), and there is little agreement during base streamflow conditions or for soil NO_3^-.

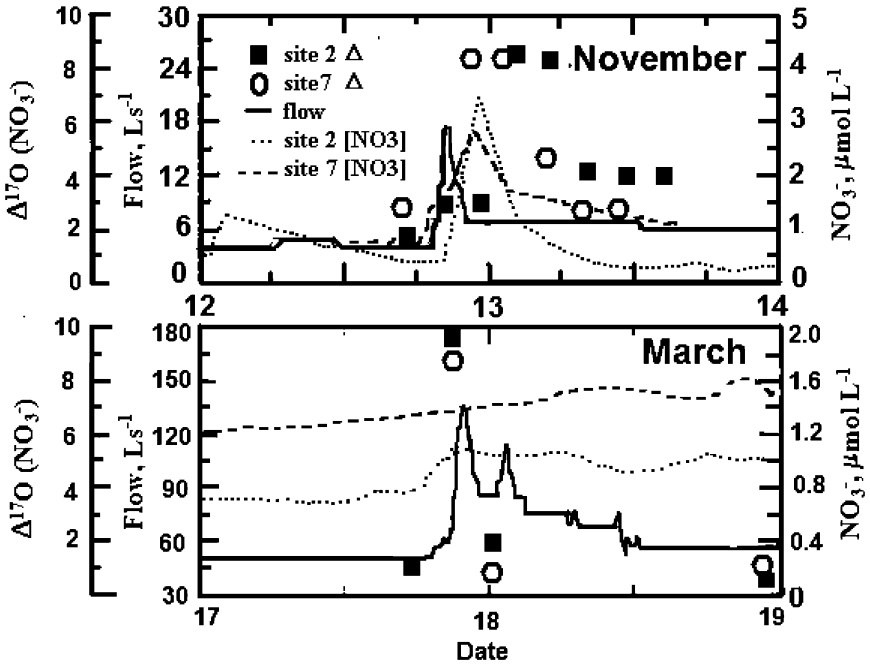

FIGURE 5. Streamflow hydrograph for Devil Canyon (solid line), stream NO_3^- concentration for site 2 (dotted line) and site 7 (dashed line), and $\Delta^{17}O$ variations for site 2 (■) and site 7 (○) during November and March rainstorms in the Devil Canyon watershed. The November storm was preceded by an 8 month dry period. The March storm came at the end of the rainy season.

the soil. The stream samples also showed that $NO_3^-{}_{atm}$ transported through soil and groundwater in the catchments did not undergo complete biological processing. At the high-deposition locations (San Dimas and Devil Canyon) the stream base flow $NO_3^-{}_{atm}$ was approximately twice that of moderate-pollution regions (San Gorgonio). These base flow NO_3^- $\Delta^{17}O$ values are not the result of $NO_3^-{}_{atm}$ leached into the streams directly from soil because there is no soil/stream hydrologic connection during dry season base flow conditions. These results suggest that even groundwater in the region is contaminated by $NO_3^-{}_{atm}$ from atmospheric deposition.

Although we did not analyze changes in $\Delta^{17}O$ values of soil NO_3^- over a detailed time frame, it should be noted the potential use of $\Delta^{17}O$ as a tool in understanding soil N cycling. Since processes such as uptake, utilization, and denitrification leave $\Delta^{17}O$ conserved, changes in soil $\Delta^{17}O$ must be the result of net nitrification. This has implications for researchers interested in N cycling who are currently studying polluted sites or who are conducting controlled experiments using expensive ^{15}N-enriched materials. Natural nitrate fertilizer imported from the Atacama region of northern Chile has been determined to have $\Delta^{17}O \approx 20‰$ since it is derived from millennial scale deposition of $NO_3^-{}_{atm}$ (*26*, *34*). This

readily available fertilizer offers a low-cost alternative to ^{15}N for a tracing nitrification dynamics and the fate of NO_3^- as it cycles within ecosystems.

Stream NO_3^- Isotope Dynamics during Storm Conditions. The Devil Canyon watershed was also sampled during two storm events, at two locations (Figure 5). Site 2 is in the lower part of the watershed and representative of the total watershed flux, and site 7 is one small seasonal tributary in the lower section of the watershed. For both storms during peak flow, close to 40% of the stream NO_3^- originates from atmospheric sources. The NO_3^- $\delta^{18}O$ values differ by 10‰ between locations during storm 1 (Table 1), indicating that nitrification/denitrification or some unmeasured isotope effects are locally altering the $\delta^{18}O$, but $\Delta^{17}O$ data signify that it is not a decrease in the relative amount of $NO_3^-{}_{atm}$. The data indicate that during the dry period prior to storm 1, $NO_3^-{}_{atm}$ accumulated on plant and soil surfaces. At the onset of the rainy season, the nitrate is rapidly leached through the dry soil to the shallow groundwater, with little time for the surface $NO_3^-{}_{atm}$ to undergo biotic or abiotic processes that can induce isotopic fractionation, before being discharged into the stream. This description accounts for the parallel $\Delta^{17}O$ and NO_3^- concentration maximums during the initial rains (Figure 5). Silicon concentrations during this first storm were greatly depleted (<1 ppm) relative to base flow conditions (~11 ppm), supporting the shallow groundwater hypothesis. The source of the additional $NO_3^-{}_{atm}$ is not the precipitation itself, since anion analysis of the rainwater gave a NO_3^- concentration of ~1 ppm, which is equal to base flow concentrations. The weak NO_3^-/biotic interaction is also evident in the NO_3^- $\delta^{18}O$ values, which are in agreement with $NO_3^-{}_{atm}$ loading on the basis of the $\Delta^{17}O$ values (Figure 4), and have been observed in other regions with high N deposition and low N interaction with the soil (*10*, *27*).

The absence of an increase in the stream NO_3^- concentration during storm 2 suggests most of the NO_3^- in the soil and vegetation has been flushed by previous rains and is either exported or consumed by biological processes. The coincident streamflow and NO_3^- $\Delta^{17}O$ peaks are likely the result of base flow NO_3^- and precipitation $NO_3^-{}_{atm}$ mixing. During March the base flow is ~10 times as great as that observed during November. The silicon concentrations during the March storm (~8 ppm) did not dramatically decrease relative to the base flow concentrations (~11 ppm) as was observed during the November storm, indicating that deep groundwater from the rising water table was of greater influence during the time of the year. This would explain the rapid return in NO_3^- $\Delta^{17}O$ values to their base flow values, a phenomenon not observed in the November storm where shallow groundwater is more important after the long dry period.

These observations demonstrate that, with more complex nutrient cycling and hydrographic dynamics, $\delta^{18}O$ becomes less robust as a $NO_3^-{}_{atm}$ tracer, while the $\Delta^{17}O$ tracer is conserved. This supposition is evident in the two soil lysimeter NO_3^- samples where the $\delta^{18}O$ values differ by 40‰, yet the $\Delta^{17}O$ values are identical within the experimental error of each other (Table 1). The large percent of $NO_3^-{}_{atm}$ observed in soil samples conclusively shows that increases in soil NO_3^- observed in the soils of southern California ecosystems impacted by air pollution are a direct result of atmospheric deposition. This result is important since increased soil nitrogen concentrations are correlated with ecosystem changes that have been observed in southern California.

Finding so large a fraction (4−40%) of unassimilated atmospherically derived NO_3^- in runoff at all sites and the very high percentages (20−40%) in storm runoff in the Devil Canyon catchment has important implications for terrestrial ecology. These results indicate a direct connection between NO_3^- concentrations in streamwater and the rate of atmospheric N deposition, although postdepositional processing of N within the watershed is also a major factor influencing runoff NO_3^- concentrations. The large amounts of $NO_3^-{}_{atm}$ in runoff imply that previous estimates of the fraction of $NO_3^-{}_{atm.}$ in streams from N-impacted regions may be too conservative (*35*) in some instances and that some terrestrial ecosystems may not be as efficient in retaining atmospheric N deposition as formerly expected. In particular, seasonally dry ecosystems may leach substantial amounts of inorganic N, especially at the onset of winter rains as seen in our results. This leaching is likely to also impact groundwater and base flow NO_3^- concentrations. This study clearly demonstrates that using $\Delta^{17}O$ signatures to trace the fate of atmospheric nitrate is a powerful technique and can augment the $\delta^{18}O$ and $\delta^{15}N$ dual isotope method (*10*, *11*). This will increase our understanding of N processing and N retention efficiencies within ecosystems that are impacted by atmospheric N deposition.

Literature Cited

(1) Galloway, James N. *Environ. Pollut.* **1998**, *102*, 15−24.
(2) Vitousek, P. M.; Aber, J. D.; Howarth, R. W.; Likens, G. E.; Matson, P. A.; Schindler, D. W.; Schlesinger, W. H.; Tilman, D. G. *Ecol. Appl.* **1997**, *7*, 737−750.
(3) Howarth, R. W.; Billen, G.; Swaney, D.; Townsend, A.; Jaworski, N.; Lajtha, K.; Downing, J. A.; Elmgren, R.; Caraco, N. *Biogeochemistry* **1996**, *35*, 75−139.
(4) Tilman, D.; Wedin, D.; Knops, J. *Nature* **1996**, *379*, 718−720
(5) Fenn, M. E.; Poth, M. A.; Aber, J. D.; Baron, J. S.; Bormann, B. T.; Johnson, D. W.; Lemly, A. D.; McNulty, S. G.; Ryan, D. E.; Stottlemyer, R. *Ecol. Appl.* **1998**, *8*, 706−733.
(6) Paerl, H. W.; Boynton, W. R.; Dennis, R. L.; Driscoll, C. T.; Greening, H. S.; Kremer, J. N.; Rabalais, N.; Seitzinger, S. P. *Nitrogen loading in coastal water bodies: an atmospheric perspective*; American Geophysical Union: Washington, DC, 2001; pp 11−52.
(7) Williams, M. W.; Baron, J. S.; Caine, N.; Sommerfeld, R.; Sanford, R. *Environ. Sci. Technol.* **1996**, *30*, 640−646.
(8) Stoddard, J. L. *Environ. Chem. Lakes Reservoirs, 1991* **1994**, 223−284.
(9) Seinfeld, J. H.; Pandis, S. N. *Atmospheric chemistry and physics: from air pollution to climate change*; Wiley: New York, 1998.
(10) Durka, W.; Schulze, E. D.; Gebauer, G.; Voerkelius, S. *Nature* **1994**, *372*, 765−767.
(11) Kendall, C. *Isot. Tracers Catchment Hydrol.* **1998**, 519−576.
(12) Mayer, B.; Bollwerk, S. M.; Mansfeldt, T.; Hutter, B.; Veizer, J. *Geochim. Cosmochim. Acta* **2001**, *65*, 2743−2756.
(13) Michalski, G.; Scott, Z.; Kabiling, M.; Thiemens, M. *Geophys. Res. Lett.* **2003**, *30*, ASC 14−1-.
(14) Thiemens, M. H.; Savarino, J.; Farquhar, J.; Bao, H. *Acc. Chem. Res.* **2001**, *34*, 645−652.
(15) Morton, J.; Barnes, J.; Schueler, B.; Mauersberger, K. *J. Geophys. Res., [Atmos.]* **1990**, *95*, 901−907.
(16) Young, E. D.; Galy, A.; Nagahara, H. *Geochim. Cosmochim. Acta* **2002**, *66*, 1095−1104.
(17) Bytnerowicz, A.; Miller, P. R.; Olszyk, D. M. *Atmos. Environ.* **1987**, *21*, 1749−1757.
(18) Riggan, P. J.; Lockwood, R. N.; Lopez, E. N. *Environ. Sci. Technol.* **1985**, *19*, 781−789.
(19) Fenn, M. E.; Haeuber, R.; Tonnesen, G. S.; Baron, J. S.; Grossman-Clarke, S.; Hope, D.; Jaffe, D. A.; Copeland, S.; Geiser, L.; Rueth, H. M.; Sickman, J. O. *Bioscience* **2003**, *53*, 391−403.
(20) Egerton-Warburton, L. M.; Graham, R. C.; Allen, E. B.; Allen, M. F. *Proc. R. Soc. London, Ser. B* **2001**, *268*, 2479−2484.
(21) Padgett, P. E.; Allen, E. B. *Plant Ecol.* **1999**, *144*, 93−101.
(22) Meixner, T.; Fenn, M.; Poth. *TheScientificWorld* [online computer file] **2001**, 1.
(23) Fenn, M. E.; Poth, M. A. *J. Environ. Qual.* **1999**, *28*, 822−836.
(24) Fenn, M. E.; Poth, M. A.; Schilling, S. L.; Grainger, D. B. *Can. J. For. Res.* **2000**, *30*, 1476−1488.
(25) Appel, B. R.; Wall, S. M.; Tokiwa, Y.; Haik, M. *Atmos. Environ.* **1979**, *13*, 319−325.
(26) Michalski, G.; Savarino, J.; Böhlke, J. K.; Thiemens, M. *Anal. Chem.* **2002**, *74*, 4989−4993.
(27) Burns, D. A.; Kendall, C. *Water Resour. Res.* **2002**, *38*, Article No. 1051.
(28) Lyons, J. R. *Geophys. Res. Lett.* **2001**, *28*, 3231−3234.
(29) Johnston, J. C.; Thiemens, M. H. *J. Geophys. Res., [Atmos.]* **1997**, *102*, 25395−25404.

(30) Revesz, K.; Böhlke, J. K. *Anal. Chem*. **2002**, *74*, 5410−5413.
(31) Mayer, B.; Boyer, E. W.; Goodale, C.; Jaworski, N. A.; van Breemen, N.; Howarth, R. W.; Seitzinger, S.; Billen, G.; Lajtha, K.; Nadelhoffer, K.; Van Dam, D.; Hetling, L. J.; Nosal, M.; Paustian, K. *Biogeochemistry* **2002**, *57*, 171−197.
(32) Padgett, P. E.; Allen, E. B.; Bytnerowicz, A.; Minich, R. A. *Atmos. Environ*. **1999**, *33*, 769−781.
(33) Bytnerowicz, A.; Miller, P. R.; Olszyk, D. M.; Dawson, P. J.; Fox, C. A. *Atmos. Environ*. **1987**, *21*, 1805−1814.
(34) Michalski, G.; Böhlke, J. K.; Thiemens, M. H. *Geochim. Cosmochim. Acta*, accepted for publication.
(35) Whitall, D.; Hendrickson, B.; Paerl H. *Environ. Int.* **2003**.

Received for review September 5, 2003. Revised manuscript received January 21, 2004. Accepted January 28, 2004.

ES034980+